



LAWRENCE
LIVERMORE
NATIONAL
LABORATORY

LLNL-JRNL-869469

Emerging multiscale insights on microbial carbon use efficiency in the land carbon cycle

X. He, E. Abs, S. D. Allison, F. Tao, Y. Huang, S. Manzoni, R. Abramoff, E. Bruni, S. Bowring, A. Chakrawal, P. Ciais, L. Elsgaard, P. Friedlingstein, K. Georgiou, G. Hugelius, L. Holm, W. Li, Y. Luo, G. Marmasse, N. Nunan, C. Qiu, S. Sitch, Y. P. Wang, D. S. Goll

September 18, 2024

Nature Communications

Disclaimer

This document was prepared as an account of work sponsored by an agency of the United States government. Neither the United States government nor Lawrence Livermore National Security, LLC, nor any of their employees makes any warranty, expressed or implied, or assumes any legal liability or responsibility for the accuracy, completeness, or usefulness of any information, apparatus, product, or process disclosed, or represents that its use would not infringe privately owned rights. Reference herein to any specific commercial product, process, or service by trade name, trademark, manufacturer, or otherwise does not necessarily constitute or imply its endorsement, recommendation, or favoring by the United States government or Lawrence Livermore National Security, LLC. The views and opinions of authors expressed herein do not necessarily state or reflect those of the United States government or Lawrence Livermore National Security, LLC, and shall not be used for advertising or product endorsement purposes.

1 Emerging multiscale insights on microbial carbon 2 use efficiency in the land carbon cycle

3
4 Xianjin He¹, Elsa Abs¹, Steven D. Allison^{2,3}, Feng Tao⁴, Yuanyuan Huang⁵, Stefano Manzoni⁶,
5 Rose Abramoff⁷, Elisa Bruni⁸, Simon P.K. Bowring¹, Arjun Chakrawal⁹, Philippe Ciais¹, Lars
6 Elsgaard^{10,11}, Pierre Friedlingstein^{12,13}, Katerina Georgiou¹⁴, Gustaf Hugelius⁶, Lasse Busk
7 Holm¹⁰, Wei Li¹⁵, Yiqi Luo¹⁶, Gaëlle Marmasse^{1,17}, Naoise Nunan^{18,19}, Chunjing Qiu²⁰, Stephen
8 Sitch¹², Ying-Ping Wang²¹, Daniel S. Goll^{1,*}

9
10 1 Laboratoire des Sciences du Climat et de l'Environnement, IPSL-LSCE, CEA/CNRS/UVSQ,
11 Orme des Merisiers, 91191, Gif sur Yvette, France.

12 2 Department of Ecology and Evolutionary Biology, University of California Irvine, Irvine, CA,
13 92697, USA.

14 3 Department of Earth System Science, University of California Irvine, Irvine, CA, 92697, USA.

15 4 Department of Ecology and Evolutionary Biology, Cornell University, Ithaca, NY, 14850, USA.

16 5 Key Laboratory of Ecosystem Network Observation and Modeling, Institute of Geographic
17 Sciences and Natural Resources Research, Chinese Academy of Sciences, Beijing, 100101,
18 China.

19 6 Department of Physical Geography and Bolin Centre for Climate Research, Stockholm
20 University, Stockholm SE-10691, Sweden.

21 7 Ronin Institute, Montclair, NJ, USA.

22 8 LG-ENS (Laboratoire de géologie) CNRS UMR 8538 - Ecole normale supérieure, PSL
23 University -IPSL, Paris, France.

24 9 Environmental Molecular Sciences Laboratory, Pacific Northwest National Laboratory,
25 Richland, WA 99354, USA.

26 10 Department of Agroecology, Aarhus University, 8830 Tjele, Denmark.

27 11 iCLIMATE Interdisciplinary Centre for Climate Change, Aarhus University, 4000 Roskilde,
28 Denmark.

29 12 Faculty of Environment, Science and Economy, University of Exeter, Exeter, EX4 4QF, UK.

30 13 Laboratoire de Météorologie Dynamique, Institut Pierre-Simon Laplace, CNRS, École
31 Normale Supérieure, Université PSL, Sorbonne Université, École Polytechnique, Paris, France.

32 14 Physical and Life Sciences Directorate, Lawrence Livermore National Laboratory, Livermore,
33 CA 94551, USA.

34 15 Department of Earth System Science, Ministry of Education Key Laboratory for Earth System
35 Modeling, Institute for Global Change Studies, Tsinghua University, Beijing, China.

36 16 Soil and Crop Sciences Section, School of Integrative Plant Science, Cornell University,
37 Ithaca, NY 14850, USA.

38 17 Ecole Normale Supérieure de Lyon, 69342 Lyon, France.

39 18 Institute of Ecology and Environmental Sciences – Paris, Sorbonne Université, CNRS, IRD,
40 INRA, P7, UPEC, 4 place Jussieu, 75005 Paris, France.

41 19 Department of Soil and Environment, Swedish University of Agricultural Sciences, 75007
42 Uppsala, Sweden.

43 20 Research Center for Global Change and Complex Ecosystems, School of Ecological and
44 Environmental Sciences, East China Normal University, Shanghai, China.

45 21 CSIRO Environment, Private Bag 10, Clayton South, VIC 3168 Australia.

46

47 * Corresponding author: Daniel S. Goll (dsgoll123@gmail.com)

This document was prepared as an account of work sponsored by an agency of the United States government. Neither the United States government nor Lawrence Livermore National Security, LLC, nor any of their employees makes any warranty, expressed or implied, or assumes any legal liability or responsibility for the accuracy, completeness, or usefulness of any information, apparatus, product, or process disclosed, or represents that its use would not infringe privately owned rights. Reference herein to any specific commercial product, process, or service by trade name, trademark, manufacturer, or otherwise does not necessarily constitute or imply its endorsement, recommendation, or favoring by the United States government or Lawrence Livermore National Security, LLC. The views and opinions of authors expressed herein do not necessarily state or reflect those of the United States government or Lawrence Livermore National Security, LLC, and shall not be used for advertising or product endorsement purposes.

Work at LLNL was performed under the auspices of the U.S. Department of Energy by Lawrence Livermore National Laboratory under Contract DE-AC52-07NA27344.

IM Release Number: LLNL-JRNL-869469

48 Abstract

49 Microbial carbon use efficiency (CUE) affects the fate and storage of carbon in terrestrial
50 ecosystems, but its global importance remains uncertain. Accurately modeling and predicting
51 CUE on a global scale is challenging due to inconsistencies in measurement techniques and the
52 complex interactions of climatic, edaphic, and biological factors across scales. The link between
53 microbial CUE and soil organic carbon relies on the stabilization of microbial necromass within
54 soil aggregates or its association with minerals, necessitating an integration of microbial and
55 stabilization processes in modeling approaches. In this perspective, we propose a
56 comprehensive framework that integrates diverse data sources, ranging from genomic
57 information to traditional soil carbon assessments, to refine carbon cycle models by
58 incorporating variations in CUE, thereby enhancing our understanding of the microbial
59 contribution to carbon cycling.

60 Introduction

61 Earth System Models (ESMs) are indispensable tools for predicting the planetary
62 response to climate change ¹. The accuracy and reliability of ESMs are crucial for informing
63 climate projections that guide policy decisions. Soils store more carbon (C) than plants, the
64 surface ocean or the atmosphere, and thus are critical for the functioning of the Earth system ².
65 While ESMs are becoming increasingly complex, their predictions of soil organic C (SOC)
66 stocks have improved only marginally in recent decades ^{3,4}.

67 Microbial communities process most of the C entering the soil, thereby shaping its fate
68 ^{5,6}. Microbes metabolize multiple C sources, including detritus, root exudates, and microbial
69 metabolites ⁷. The energy needed to acquire C depends on whether the compounds can be
70 taken up directly or require prior enzymatic degradation ⁸. Additionally, microbial community
71 composition and functioning are influenced by prevailing climatic conditions ^{9–11}. The general
72 omission of microbial community structure and related processes in C cycle models has been
73 suggested as one of the causes for their poor performance in predicting SOC stocks and their
74 responses to climate change ^{12,13}.

75 Recognizing the impracticality of representing every conceivable microbial metabolic
76 pathway, many models combine a spectrum of microbial processes into a single metric referred
77 to as microbial C use efficiency (CUE) ^{14,15}. CUE, as a model parameter or as a system property
78 emerging from multiple co-occurring processes, represents the fraction of C uptake allocated to
79 the production of new microbial biomass ¹⁶. Using this definition, CUE declines as more C is
80 used for respiration to generate energy (for substrate uptake, cellular maintenance, enzyme
81 production) or for exudation (extracellular enzymes, polysaccharides) ^{17,18}. This pragmatic
82 approach streamlines the modeling of soil C cycling by incorporating the diverse fates of
83 microbial C, including biomass production, respiration, and exudation, thereby providing a more
84 comprehensive understanding of microbially-mediated C-pathways.

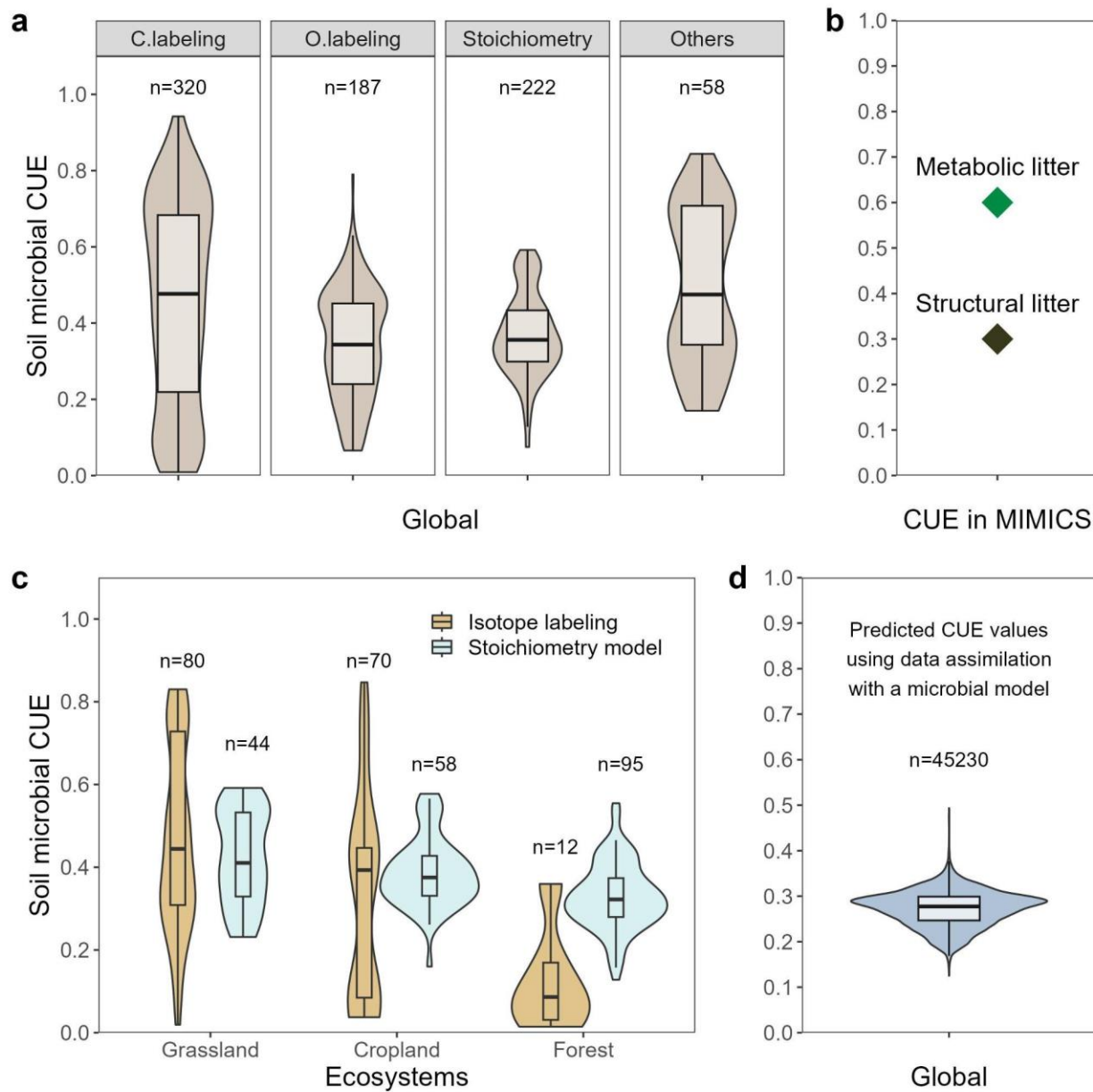
85 However, accurately integrating the spatial or temporal dynamics of microbial CUE into
86 soil C models remains a significant challenge. Most of the current C cycle models either lack
87 explicit representation of CUE or treat it as a constant value ⁴, despite our understanding that
88 CUE varies under different environmental conditions. For example, observations indicate
89 significant variability in CUE at the global scale ⁸, which may be partially attributed to
90 inconsistencies among measurement techniques (Figure 1a). Moreover, comparisons across

91 ecosystems reveal that CUE is generally higher in grasslands than in croplands, with forests
92 consistently showing the lowest CUE values, regardless of the measurement approaches used
93^{19,20} (Figure 1c). CUEs derived from data assimilation²¹ are also lower than those from more
94 direct measurement approaches (Figure 1d).

95 Several attempts have been made to reflect or incorporate CUE variations into models of
96 litter²² or soil organic matter^{9,13} decomposition with the aim of assessing the implications for
97 soil C cycling. For example, incorporating an empirically-derived negative relationship between
98 microbial CUE and temperature into a microbial-explicit SOC model improved the simulation of
99 contemporary soil C stocks²³. Zhang et al.²⁴ introduced the effects of substrate quality and soil
100 fertility on microbial respiration, highlighting the joint control of litter quality and quantity on the
101 steady-state SOC stocks. Wieder et al.²⁵ enhanced the understanding of CUE variation by
102 including two types of decomposers with differing substrate preferences and CUE (Figure 1b).
103 These examples suggest that more realistic representations of microbial C transformations have
104 the scope for improving model predictions of soil C^{23,26}. However, these predictions were poorly
105 constrained by observational data, calling their reliability into question^{21,27,28}.

106 In this Perspective, we synthesize our understanding of CUE regulatory factors and
107 databases for constraining numerical models, with the aim of clarifying complexities, addressing
108 controversies, and providing a holistic perspective on pathways to adequately reflect CUE
109 variations in C cycle models and their consequences for simulated soil C stocks.

110



111

112 **Figure 1: Variability of carbon use efficiency (CUE) at a global scale.** a): Observation-based
 113 CUE estimates at the global scale from C (^{13}C and ^{14}C) and ^{18}O isotopic labeling, stoichiometric
 114 modeling and other methods. Data were collected from ^{19,21,29–31}. b): CUE constants used in the
 115 Microbial-MIneral Carbon Stabilization model (MIMICS) for two litter types (diamonds).
 116 Metabolic litter comprises plant litter that decomposes easily, whereas structural litter is more
 117 resistant to decomposition ³². c): Observation-based estimates for different ecosystems using
 118 isotopic labeling ²⁹ or stoichiometric modeling ¹⁹. d): CUE values predicted using a microbial

119 model assimilating information on SOC profiles ²¹. Data assimilation integrates observed data
120 into predictive models to refine model parameters and improve estimation accuracy.

121

122 Data availability and challenges

123 Terminology and definitions of microbial CUE

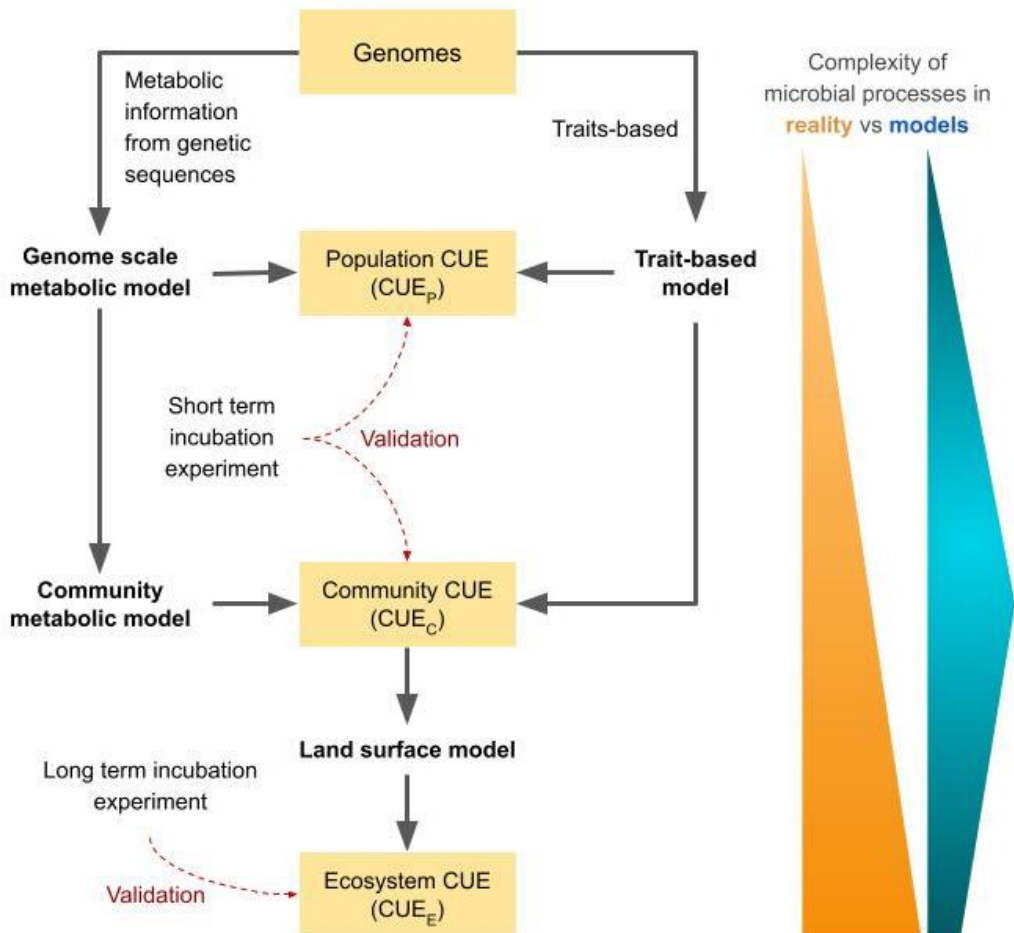
124 The concept of microbial CUE, the fraction of C uptake that is used to produce microbial
125 biomass ^{16–18}, is intuitively straightforward, but CUE definitions vary depending on the ecological
126 processes involved, measurement methods, and scales of biological organization (e.g.,
127 population, community and ecosystem) ^{14,17}. Therefore, CUE can be regarded as an emergent
128 parameter, encapsulating multiple processes within a single metric. It is useful in modeling as
129 the number of processes that can be modeled is constrained by practical limitations (e.g.
130 availability of data for calibration). Consequently, ecosystem models often simplify microbial
131 process complexity, which in reality, escalates from the genomic to the ecosystem level (Figure
132 2).

133 CUE is quantitatively expressed as the ratio of microbial growth (μ) to C uptake (U) ^{16,33},
134 that is, $CUE = \mu/U$. This ratio encapsulates the efficiency with which microorganisms convert
135 assimilated C into biomass. Microbial uptake involves C assimilation for growth (μ), respiration
136 (R), and the secretion of extracellular enzymes and metabolites (EX). Geyer et al. (2016)
137 introduced a nested conceptual framework for understanding CUE across different biological
138 organization levels: population (CUE_P), community (CUE_C), and ecosystem (CUE_E). This
139 framework is useful for integrating C fluxes mediated by soil microbes into models at various
140 ecological scales (Figure 2).

141 CUE_P reflects the species-specific functioning of microbial taxa (e.g., biosynthesis rate,
142 exudate production) and thermodynamics of C substrate metabolism that limits the proportion of
143 C uptake used for biosynthesis versus C lost from the cell (e.g., mineralized or exuded as
144 metabolites). Typically measured in cultured populations, the CUE_P formula adjusts for
145 respiration (R) and exudation (EX) losses from the uptake, expressed as $CUE_P = \frac{U - R - EX}{U}$. CUE_C
146 incorporates additional environmental and community factors influencing microbial metabolism
147 in natural communities consisting of multiple populations. It focuses on gross microbial

148 production prior to the recursive substrate recycling of necromass and exudates, capturing the
 149 metabolic response of microbial communities to substrates over short durations (hours), and is
 150 similarly expressed as $CUE_C = \frac{U-R-EX}{U}$.

151 CUE_E considers C retention as net microbial growth over longer time scales (days to
 152 months), taking into account the drivers of CUE_P and CUE_C as well as microbial biomass
 153 turnover. On these time scales, a significant proportion of microbial biomass is converted to
 154 necromass following microbial death (MD)³² such that $CUE_E = \frac{U-R-EX-MD}{U}$, encompassing all
 155 aspects of microbial C processing, including death and recycling processes.



156

157 **Figure 2. Schematic representation of a cluster of models integrating observational**
 158 **constraints on CUE at population (CUE_P), community (CUE_C) and ecosystem (CUE_E)**
 159 **scales.** The genome-scale metabolic model predicts the movement of metabolites within a cell
 160 based on its genomic information. CUE_P and CUE_C can be validated by short-term incubation
 161 measurements, while CUE_E requires long-term incubation measurements. Although the scales

162 and processes governing CUE expand from individual cells to entire ecosystems, there is a
163 practical limit to the extent they can be resolved in C cycle models.

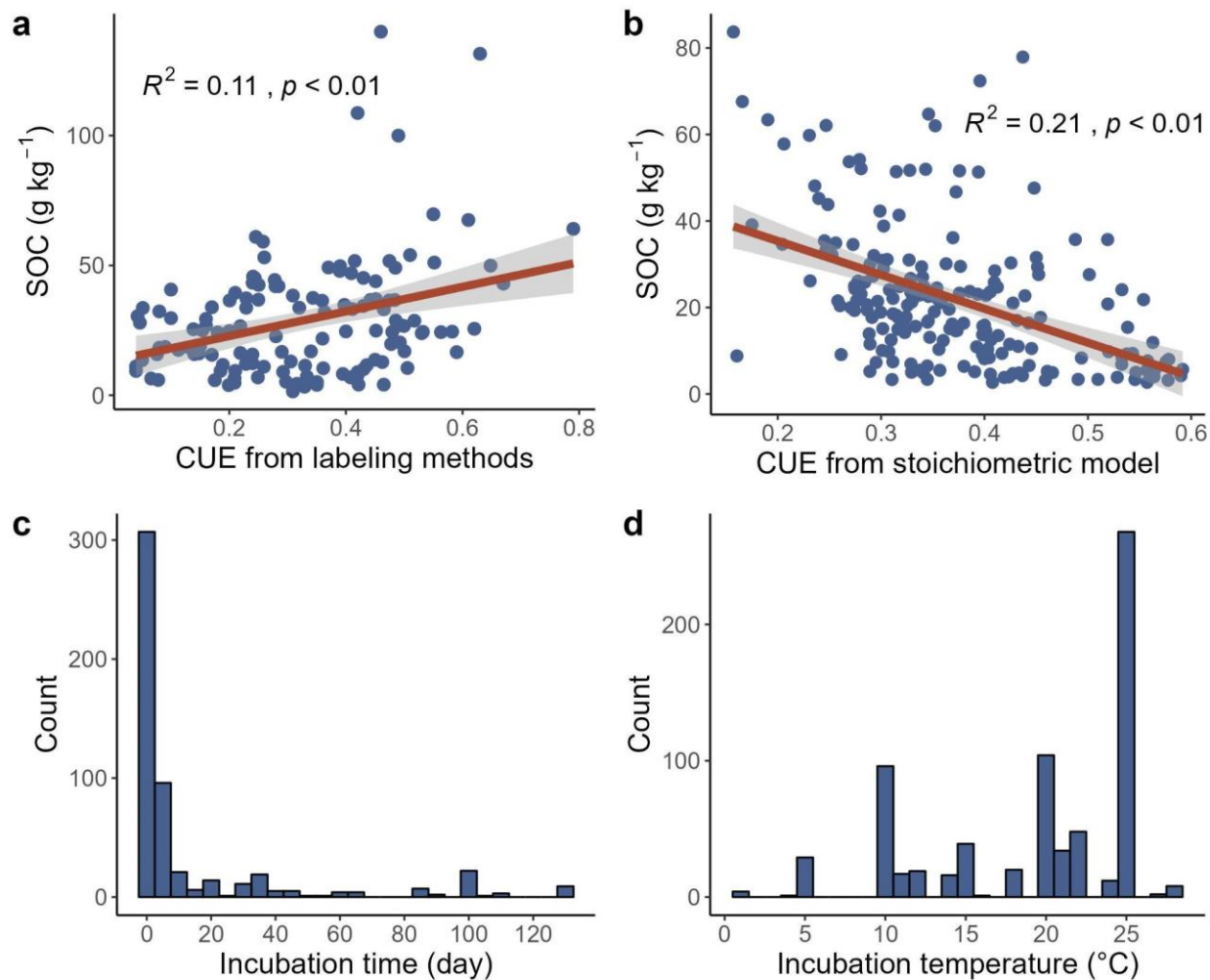
164

165 Methods for measuring microbial CUE

166 Multiple approaches can be used to quantify CUE, such as isotopically labeling
167 substrates^{35,36}, stoichiometric modeling^{22,37} and others³⁸. These methods rely on different
168 assumptions and capture distinct microbial processes, which can explain the variability in CUE
169 estimates across methods^{8,39,40} (Figure 1a), including differences in the response of CUE to
170 environmental changes⁴¹, and the relationship between CUE and SOC (Figure 3a and b).

171 The most common approach for measuring CUE is the tracking of isotopically labeled
172 compounds (¹⁴C, ¹³C labeled substrate, or ¹⁸O water) introduced to the system. Carbon isotopes
173 in microbial substrates enable the differentiation between C allocated to microbial biomass and
174 that released through respiration. Although this labeling technique is widely used, its results can
175 be influenced by the choice and combination of substrates³⁵, as well as the incubation period
176^{14,42}. A significant limitation of this approach is that measured CUE reflects only the efficiency of
177 those microbes that use the introduced substrates, not the entire microbial community.
178 Furthermore, the variation in incubation times and temperatures across different studies (Figure
179 3c and d) presents a substantial obstacle to standardizing CUE measurements.

180



181

182 **Figure 3. The relationships between soil organic carbon (SOC) concentration and CUE**
 183 **from (a) isotopic labeling methods (^{14}C , ^{13}C labeled substrate, and ^{18}O water) and (b)**
 184 **stoichiometric modeling. The figure also shows (c) the incubation duration and (d)**
 185 **temperature employed in studies using labeling and incubation methods. Data in the**
 186 **panels are from (a) ²¹, (b) ¹⁹, and (c and d) ²⁰.**

187

188 The method using ^{18}O -labeled water is based on the incorporation of the ^{18}O -atom into
 189 microbial DNA as a measure of growth as compared to catabolic C losses as CO_2 ^{36,43}. This
 190 method has higher accuracy than the C labeling method as it is not substrate specific, does not
 191 perturb microbial metabolism like methods involving substrate addition, and exhibits
 192 comparatively less variability over time³⁹. Nonetheless, this method faces limitations such as
 193 higher cost and demanding technical procedures. Concerns also arise regarding the method's

194 foundational assumptions, e.g., the presumption that water is the sole oxygen source for
195 microbial DNA synthesis and the hypothesis that all microbial cells maintain a consistent DNA to
196 biomass C ratio ⁴⁴. Furthermore, its applicability in dry soils is challenging ⁴⁵.

197 Stoichiometric modeling is a common method for indirectly estimating CUE, which is
198 based on the assumption that microbes growing on plant detritus allocate C to produce
199 enzymes and other necessary components to acquire nutrients in the appropriate elemental
200 ratios at the whole-community scale ^{33,37}. This approach offers the advantage of requiring only a
201 limited number of parameters, such as the activities of enzymes targeting C versus nitrogen (N)
202 or phosphorus (P) acquisition and the C:N:P composition of the substrate and microbial
203 biomass, which can be constrained by existing observations. However, it relies on highly
204 simplified assumptions regarding elemental ratios and C allocation ⁴⁰. This approach inherently
205 suggests lower CUE in soils with high SOC due to its focus on the metabolic costs of nutrient
206 acquisition under conditions where nutrients are scarce relative to C. This outcome (Figure 3b)
207 starkly contrasts with the positive correlation between CUE and SOC observed using isotopic
208 labeling techniques (Figure 3a), which are commonly considered to provide a more realistic
209 insight into the relationship between CUE and SOC. The isotope labeling method estimates
210 microbial growth and CUE by tracking the incorporation of labeled atoms into biomass or DNA,
211 reflecting intracellular biochemical transformations. In contrast, the stoichiometry model method
212 estimates CUE by analyzing the activities of extracellular enzymes and the stoichiometric
213 balance between organic matter and microbial biomass, focusing on extracellular metabolic
214 processes ⁴⁶. Therefore, caution is advised when comparing results obtained from these two
215 methods, even though they use the same term (CUE). We do not yet know the extent to which
216 the stoichiometric and isotope methods are comparable. Until we understand which patterns
217 can be accurately captured by the simpler stoichiometric method, we should rely on the more
218 robust ¹⁸O method for measuring actual CUE and the ¹³C method for CUE associated with
219 specific substrates.

220 In addition to the methods mentioned above, there are other less commonly used
221 approaches, including the use of ¹⁸O in water vapor to minimize impact on soil moisture ⁴⁵,
222 metabolic flux analysis ¹⁷, and calorespirometry ⁴⁷. Each method offers unique advantages and
223 faces specific limitations, grounded in their underlying assumptions and theoretical bases ³⁹⁻⁴¹.
224 These limitations not only affect the accuracy of these methods but also introduce significant
225 comparability issues. Consequently, there is an urgent need to improve current methodologies
226 and integrate innovative techniques to more accurately assess soil microbial CUE.

227

228 **Data gap**

229 Given the methodological challenges in measuring CUE in situ, field assessments of
230 microbial CUE are rare. The vast majority of existing CUE observations have been obtained
231 from lab incubations. Yet, these CUE observations remain scarce at the global scale, a situation
232 which is exacerbated by the lack of harmonization of observations from different measurement
233 approaches. For some ecosystems, observations are few or even nonexistent, including
234 ecosystems that play a critical role in the global C cycle, such as tropical rainforests, wetlands,
235 and peatlands ^{48,49}.

236 Existing CUE measurements mostly come from studies of the litter and surface mineral
237 soil ¹⁶. Thus, our understanding of microbial CUE in subsurface soil remains limited, which is
238 problematic as large amounts of C are stored in subsoils globally, and especially those of
239 wetlands and peatlands. The few existing studies indicate that microbial CUE decreases with
240 soil depth ^{50,51} and that subsurface CUE may be less sensitive to warming ³⁵ but more sensitive
241 to nutrient variations ⁵².

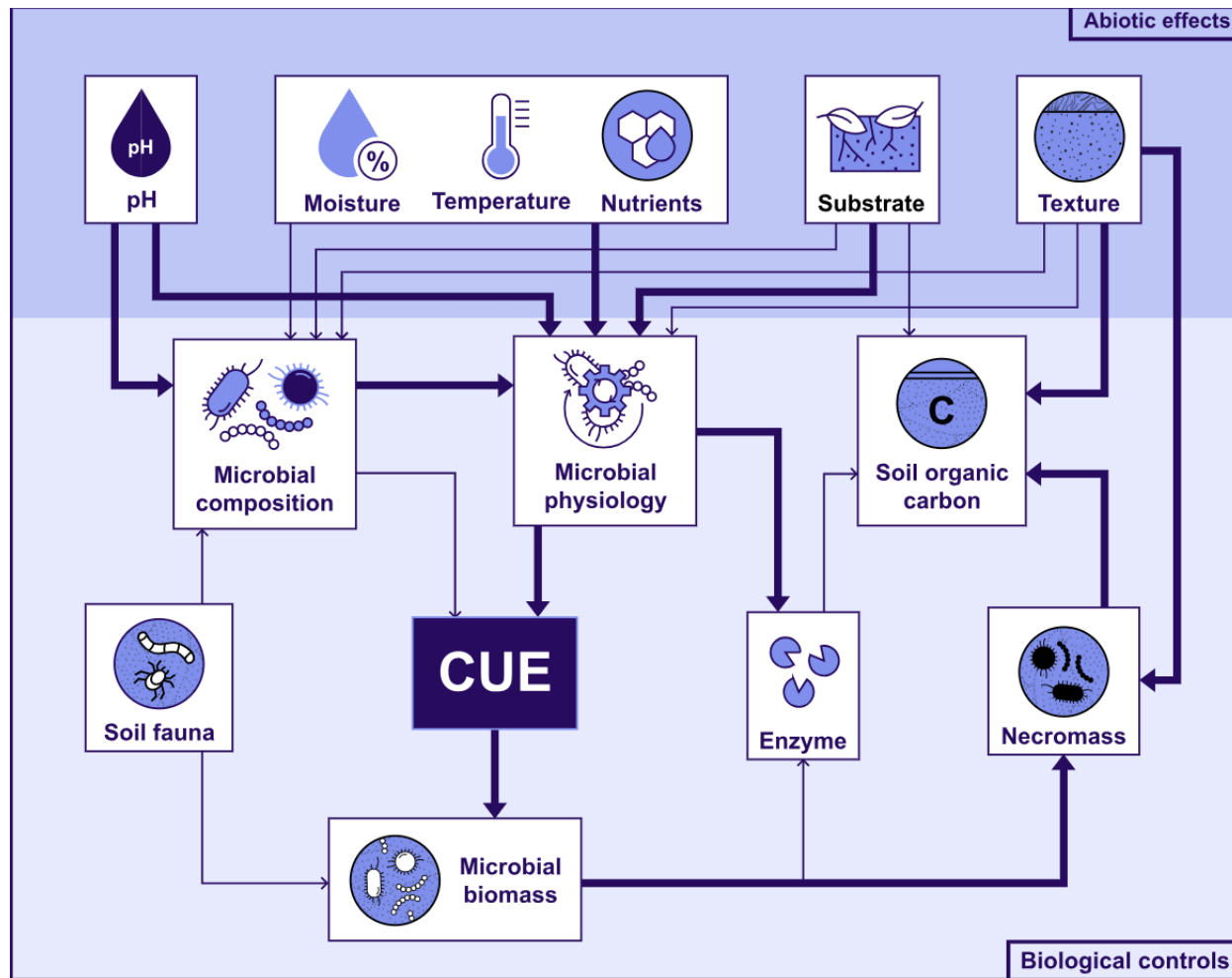
242 Moreover, data on temporal variations in CUE are lacking. A commonly overlooked
243 factor that may contribute significantly to CUE variability in soil ecosystems, regardless of
244 methodology, is seasonality in CUE. Seasonal changes are associated with significant
245 variations in substrate availability, temperature and moisture, all of which may have a
246 substantial impact on the growth and respiration of soil microorganisms, thereby altering
247 microbial CUE ⁴³. For example, CUE estimated using the ¹⁸O incorporation method ranged from
248 0.1 to 0.7 in soils from an agricultural field site and from 0.1 to 0.6 at a forest site within one year
249 ³¹. It has also been reported that soil microbial CUE exhibits significant fluctuations within a
250 short period (daily) after rewetting ^{53,54}. This temporal dynamic in CUE values could contribute to
251 the significant variability observed in CUE measurements.

252

253 **Regulatory factors governing microbial CUE**

254 The incorporation of soil microbial CUE dynamics into process-based models
255 necessitates a comprehensive understanding of a range of regulatory factors influencing CUE

256 (Figure 4). CUE at a specific biological level is influenced by features of both the microbial
 257 community itself (biological controls) and its external environment (abiotic controls). These
 258 factors frequently interact, particularly at the community and ecosystem levels: abiotic controls
 259 can modify CUE_C or CUE_E by regulating biological controls, while biological controls may induce
 260 adaptation to abiotic factors, thereby influencing the impact of abiotic controls.



261
 262 **Figure 4. Framework of biological and abiotic determinants of CUE in a carbon cycle**
 263 **context.** The darker-colored area in the figure indicates biological controls; the lighter-colored
 264 area indicates abiotic effects. The arrows depict implicit relationships and the width of the
 265 arrows corresponds to the levels of scientific certainty: confident assertions are represented by
 266 thick lines, while less confident assertions are indicated by thinner lines. These confidence
 267 levels are based on the expertise of the authors.

268

269 Biological controls:

270 Microbial physiological state

271 Microbial CUE reflects the physiological state of microorganisms. Under natural
272 conditions, only a small proportion (values vary from 1% to >20% in different studies^{55,56}) of soil
273 microbial cells are metabolically active, and soil respiration primarily originates from these
274 metabolically active cells⁵⁶. Nonetheless, a high fraction of microbial cells in the soil are in a
275 potentially active state (10 to 60% of the total microbial biomass), meaning that they are ready
276 to start using available substrates within a few hours after easily available substrate is added.
277 The shifts in physiological states of these microbial cells, resulting from changes in temperature,
278 moisture, or substrate availability, significantly impact CUE⁵⁷. Consequently, CUE_P or CUE_C
279 measurement methods relying on substrate addition may overestimate CUE¹⁴, and shifts in
280 physiological state can lead to seasonal variations in CUE³¹.

281 Microbial community diversity and composition

282 Increased microbial diversity enriches the spectrum of metabolic functions within a
283 community, potentially leading to greater microbial growth⁵⁸ and CUE_C by facilitating more
284 efficient use of varied C sources^{10,59}. The composition of microbial communities, notably the
285 ratio of fungal to bacterial biomass (F:B), plays a critical role in determining CUE_C⁶⁰.
286 Communities dominated by fungi can show higher CUE_C, attributed to their higher biomass C to
287 N ratios (C:N) and their proficiency in decomposing complex organic materials⁶¹, or lower CUE
288 due to the high costs associated with resource acquisition by decomposer fungi⁶⁰. Therefore,
289 this contrasting evidence from plant litter studies indicates that the relationship between F:B
290 ratio and CUE is context-dependent^{60,62}. Alternatively, an approach categorizing
291 microorganisms into copiotrophs (*r*-strategists with low CUE) versus oligotrophs (*K*-strategists
292 with high CUE) has been promising for estimating CUE⁶³. For example, shifts from *r*-strategists
293 to *K*-strategists explain increased CUE_C along a successional gradient in the southeastern
294 Tibetan Plateau⁶⁴.

295 Changes in community composition may also enable microbial communities to alter their
296 CUE in response to environmental changes or fluctuations^{65,66}. For instance, long-term
297 warming experiments indicate a decline in the temperature sensitivity of CUE_C, suggesting that
298 shifts in microbial composition can maintain CUE_C despite changes in temperature and

299 substrate quality³⁵. Similarly, modeling studies suggest that changing microbial community
300 composition can reduce the sensitivity of CUE_C to substrate quality⁶⁷ and soil moisture
301 fluctuations⁶⁸.

302 Biotic interactions

303 In the soil food web, biotic interactions such as mutualism, facilitation, competition, and
304 predation can shape CUE_C⁵⁹. Interspecific microbial competition drives accelerated growth
305 rates, accompanied by the release of secondary metabolites that can negatively affect CUE_C⁶⁹.
306 Antagonistic interactions may trigger stress responses, further diminishing CUE_C⁷⁰. Conversely,
307 facilitation enhances CUE_C by broadening species-realized niches, alleviating environmental
308 stress, and reducing extracellular enzyme production costs⁶⁷. Biotic interactions at higher
309 trophic levels, such as predation, can variably affect CUE_C by altering microbial density and
310 influencing the outcomes of interspecific competition^{71,72}.

311

312 Abiotic controls:

313 Temperature

314 Temperature significantly affects soil microbial CUE, with respiration often increasing
315 more than growth in short-term incubations, resulting in a decrease in CUE_P^{9,38,73}. The impact
316 on CUE_C and CUE_E is less clear⁶⁶, likely due to varied responses among microbial taxa^{74,75} and
317 interactive effects with other environmental factors^{42,43,50,76}. Temperature shifts can lead to
318 changes in community traits or select for taxa with distinct life strategies, known as trait
319 modification and trait filtering, respectively^{77,78}. However, limited research on how CUE_P varies
320 among different taxa in response to temperature impairs our ability to accurately predict
321 changes in CUE_C⁷⁹⁻⁸¹.

322 The interplay between direct and indirect temperature effects on soil microbial CUE_C and
323 CUE_E complicates our understanding of the impact of warming on CUE. Warming can intensify
324 C-nutrient imbalances, potentially diminishing microbial CUE⁸², but it can also improve the
325 efficiency of substrate utilization, thereby enhancing CUE^{36,75}. Expected reductions in soil
326 moisture due to increased evapotranspiration under warming conditions⁸³ add another layer of
327 complexity, with the combined impacts of temperature and moisture on microbial CUE

328 remaining inadequately explored^{10,84}. Some soil C models, including Millennial⁸⁵ and MIMICS²⁵
329 have begun to account for the temperature dependency of CUE_C , indicating a growing
330 recognition of the importance of including the dynamic response of microbial CUE to fluctuations
331 in temperature.

332 Soil water availability

333 Increased soil moisture promotes microbial growth and CUE by improving substrate
334 diffusivity and accessibility, and lowering investment in osmolyte synthesis, as long as
335 conditions remain oxic^{8,10,86}. Prolonged water stress reduces soil substrate accessibility and
336 increases the need to synthesize osmolytes to survive during dry periods, leading to lower
337 CUE_C ⁸⁶, even though the taxa that remain active in dry conditions can maintain relatively high
338 growth rates⁸⁷. Furthermore, drought reduces plant C inputs to the soil⁸⁶, thus potentially
339 leaving microbes with fewer lower resources, resulting in lower CUE. The intricate interplay of
340 drought-induced changes in microbial respiration and growth may leave CUE unchanged if the
341 affected processes balance each other⁸¹. High levels of soil moisture may also reduce microbial
342 CUE. As soil pores fill with water, air spaces and oxygen diffusivity decline, potentially leading to
343 anaerobic conditions if saturation occurs. Under O_2 limitation, soil microbes shift from aerobic to
344 anaerobic respiration or fermentation, significantly reducing energy yield and leading to
345 decreased microbial growth and CUE while having little impact on CO_2 production rate due to
346 upregulated biochemical rates⁸⁶.

347 Microbial responses to rewetting of a dry soil also cause rapid changes in CUE, as
348 shown in modeling studies⁵³ and confirmed by empirical evidence⁵⁴. Upon rewetting,
349 respiration increases while growth lags behind, especially when the soil has been dry for a long
350 period⁵⁴. As a result, just after rewetting, CUE is low and then increases as growth recovers
351 during the first days after rewetting. However, after this initial pulse of microbial activity, CUE
352 peaks and decreases again as substrates released during rewetting are consumed⁵⁴.

353 Nutrient availability

354 The availability of nutrients such as N and P significantly affects microbial growth and
355 respiration according to the concept of stoichiometric homeostasis which assumes constrained
356 biomass C:N:P ratios of microbial cells^{33,67}. Consequently, CUE decreases with increasing
357 substrate C-to-nutrient ratios and increases with nutrient amendment when organic substrates

358 are nutrient-poor^{22,33}. Several C cycle models, such as the one proposed by Manzoni et al.⁸⁸
359 and its later implementation²⁴, have integrated CUE dynamics as a function of stoichiometry. In
360 contrast to the homeostasis concept, recent findings highlight the capability of microbes to store
361 and use nutrients dynamically, contributing to a stable CUE across different environments by
362 separating growth and respiration processes from immediate nutrient availability⁸⁹. This
363 resilience to nutrient stress suggests that future C modeling should incorporate microbial
364 nutrient storage dynamics for enhanced predictive accuracy.

365 Soil pH

366 Soil pH influences microbial CUE_C and CUE_E by affecting the bacterial community
367 composition and acting as a potential stressor⁹⁰. It also impacts CUE by altering microbial
368 community composition⁹¹, nutrient solubility⁸⁶, and metal toxicity (e.g., aluminum⁹⁰). Habitats
369 with neutral pH generally have higher bacterial diversity and biomass compared to acidic or
370 alkaline soils⁷. The response of community composition to a shift in soil pH from acidic to
371 neutral corresponded with a significant increase in CUE_C^{90,92}. However, recent research
372 indicates a complex interplay between soil pH, microbial community composition, and CUE
373 dynamics, evidenced by both negative correlations⁹³ and a U-shaped response curve,
374 pinpointing a critical threshold at pH 6.4⁹³, although the calculations to document this are
375 complex and may necessitate refinement.

376 Soil texture and structure

377 Microbial growth is intricately linked to substrate accessibility, which is influenced by soil
378 environmental conditions like texture and soil structure. Approximately 40–70% of soil bacteria
379 are associated with microaggregates and clay particles⁹⁵. The structural complexity of the soil
380 environment also plays a crucial role in shaping the community structure and function of soil
381 microorganisms at the ecosystem level⁹⁶. Heterogeneity of soil structure and composition
382 creates diverse microhabitats that influence microbial interactions, diversity, distributions, and
383 activity, as well as ecosystem processes like nutrient cycling and organic matter decomposition
384⁹⁷. Still, limited information exists on the relationship between soil texture or structure and
385 microbial CUE. A recent meta-analysis found a significant positive link between microbial CUE_C
386 or CUE_E for glucose and soil clay content³⁰, which was attributed to increased clay content
387 enhancing substrate adsorption⁹⁸, thereby limiting substrate availability to microbes⁹⁹, and
388 resulting in higher microbial CUE_C or CUE_E.

389 Substrate quality

390 Substrate quality, defined by the chemical characteristics of organic matter that influence
391 its decomposability, such as the C:N ratio and molecular composition, significantly impacts soil
392 microbial CUE¹⁰⁰. A "high-quality" substrate typically has a lower C:N ratio, indicating a
393 balanced N content relative to C, and a lower content of recalcitrant compounds, which
394 generally leads to faster decomposition and higher CUE by providing C and nutrients that
395 microbes require for growth and metabolism⁸. Compounds requiring multiple enzymatic steps
396 for degradation can lead to reduced efficiency in building biomass. Polymeric substrates like
397 lignin and cellulose need depolymerization before cellular uptake, whereas smaller substrates
398 readily diffuse across membranes⁶⁵. Takriti et al. (2018) found a positive association between
399 soil CUE_C and ratios of cellulase to phenol oxidase enzyme activity potential, which was
400 considered to be indicative of soil organic matter (SOM) substrate quality⁵⁰. Different substrates
401 necessitate distinct metabolic pathways, resulting in different respiration rates per unit C
402 assimilated^{8,101}. Frey et al. (2013) observed lower microbial CUE_C when soils were amended
403 with oxalic acid or phenolic compounds compared to glucose, despite similar molecular sizes³⁵.

404 Microbial CUE increases with the chemical energy per mole of C in the substrate,
405 highlighting the importance of substrate chemistry for microbial CUE variability in soil⁸. This
406 relationship is akin to the concept of energetic imbalance¹⁰², which parallels the idea of
407 stoichiometric imbalance. The energy content of soil microbial biomass and substrate can be
408 quantified by the degree of reduction (γ), which refers to the average number of electrons
409 available per C atom for biochemical reactions, indicating the energy density of the substrate or
410 biomass⁸. The degree of reduction of soil microbial biomass (γ_B) is typically around 4.2, while
411 that of substrate (γ_S) usually varies between 1 (e.g., for oxalate) and 8 (methane)⁸. Most of the
412 substrates used by soil microorganisms have a γ_S of 3 (e.g., various organic acids), 4 (e.g.,
413 glucose and other carbohydrates), and rarely 5 or higher (e.g., leucine, polyhydroxyalkanoates
414 or lipids)⁸. When γ_S is lower than γ_B , the substrate's energy content is insufficient to meet
415 microbial demand, necessitating the oxidation of more substrate per unit of C assimilated,
416 thereby reducing CUE¹⁰³. These insights form the basis of the stoichiometric modeling for
417 indirect CUE estimates.

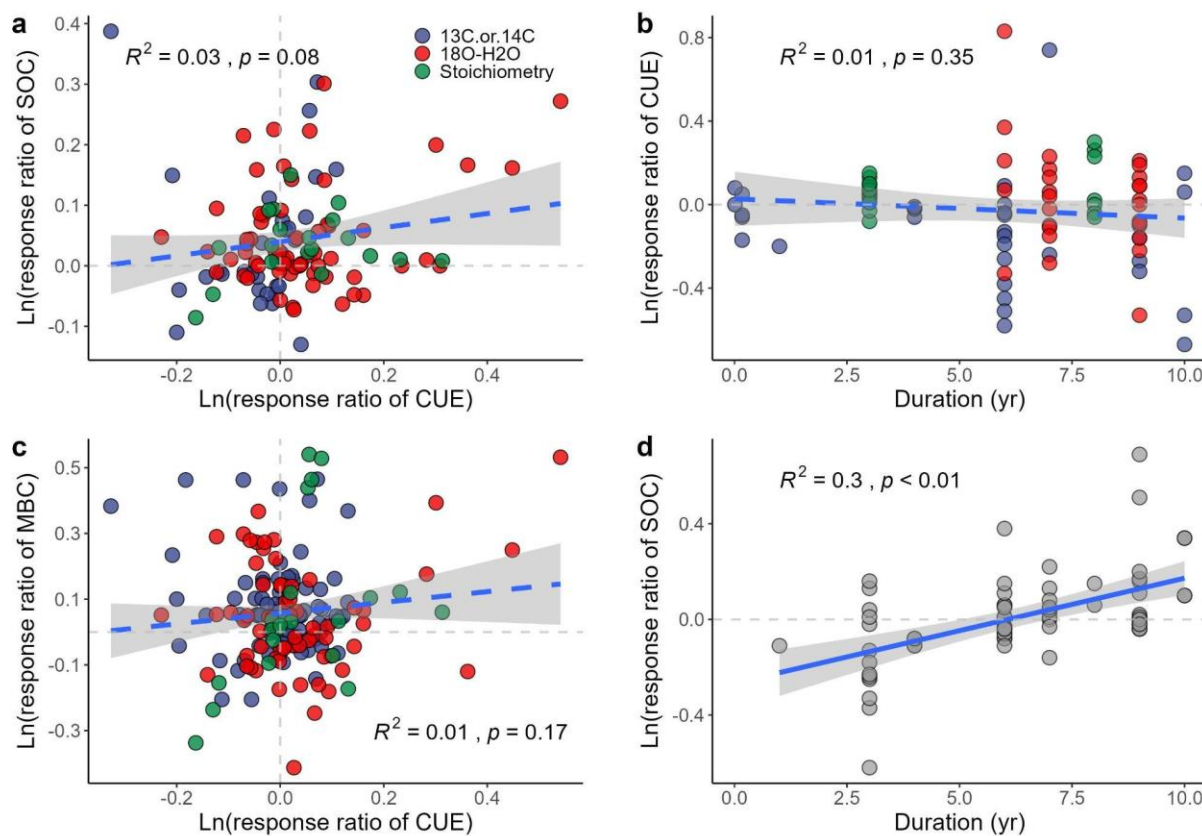
419 SOC-CUE relationship

420 The relationship between CUE and SOC concentration at the ecosystem level can be
421 positive, negative, or non-existent, depending on the interactions among multiple processes
422 21,95,98,104–106. Higher CUE can lead to increased SOC through biosynthesis and accumulation of
423 microbial by-products — facilitating SOC formation via the entombing effect 16,104,107 — or
424 conversely, trigger SOC decline through the priming effect by ramping up microbial biomass and
425 enzyme activity 9. While some studies suggest a negative correlation between CUE and SOC
426 105,106,108, the majority of research supports a positive relationship 21,77,109,110, indicating that
427 higher CUE is often linked to increased SOC levels. In a recent study, Tao et al. 21 employed
428 observational data and data assimilation algorithms and found that, on a global scale, CUE is
429 positively correlated with SOC concentration, arguing for CUE as the major determinant for
430 SOC formation. However, subsequent arguments have raised methodological concerns which
431 might have obscured the importance of microbial community dynamics 27 and SOC stabilization
432 processes 111.

433 Indeed, the link between microbial CUE and SOC is contingent upon the stabilization of
434 microbial necromass within soil aggregates or its association with minerals 98,104,107. This
435 stabilization process, pivotal for enhancing SOC, is significantly influenced by physico-chemical
436 soil properties, which vary greatly and determine the potential for necromass protection 112,113.
437 Positive SOC-CUE relationships could be anticipated in soils with high physicochemical C
438 stabilization potential and microbial communities that convert simple chemical substrates into
439 necromass 113. Conversely, when soil microbes face environmental stress, the relationship
440 between CUE and SOC becomes less predictable. Particularly under conditions where nutrients
441 are limited relative to carbon, the increased microbial respiration required to maintain
442 stoichiometric balance leads to a decreased CUE 33,37. Further reductions in CUE may be driven
443 by environmental challenges such as low oxygen or pH 91,108, as well as the physiological costs
444 of microbial competition 69. However, these stressors on microbial activity may differently affect
445 SOC, potentially leading to either a negative or negligible correlation between CUE and SOC
446 108. It's worth noting that in organic-rich soils, such as peat, C stabilization relies more on the
447 accumulation of undecomposed plant material than on necromass formation 114, making the link
448 between CUE and SOC less direct. Therefore, the CUE-SOC relationship in organic soils is
449 expected to differ from mineral soils where C is mainly stabilized by mineral associations.

450 Additionally, it is important to recognize the distinct sensitivities of microbial CUE and
 451 SOC to environmental changes, as their responses are not synchronized. Microbial CUE can
 452 adjust rapidly, from days to months, in contrast to SOC, which may take years or even decades
 453 to respond to a measurable extent^{31,115}. Data from two meta-analyses highlight this disparity,
 454 showing that although fertilization positively affects both CUE_C and SOC^{29,41}, the response
 455 ratios of CUE_C were not significantly correlated with the response ratios of SOC, or even
 456 microbial biomass C content (Figure 5a and c). Here, the "response ratio" is calculated as the
 457 ratio of the measured value in the treatment to the value in the control. Furthermore, the
 458 response ratios of microbial CUE_C were not significantly related to treatment duration (within ten
 459 years of treatment) (Figure 5b), whereas the response ratios of SOC increased significantly with
 460 experiment duration (Figure 5d). Therefore, SOC gradually approaches a new equilibrium over
 461 several decades, whereas CUE achieves equilibrium almost immediately. This discrepancy
 462 underscores the importance of considering the state (SOC and microbial biomass) dynamics of
 463 an ecosystem when evaluating the interplay between microbial CUE and SOC dynamics.

464



465

466 **Figure 5. Contrasting responses of SOC and CUE to fertilization.** Correlations between In-
467 transformed response ratios of microbial CUE and In-transformed response ratios of (a) SOC
468 and (c) microbial biomass C (MBC); and the correlation between experiment duration and In-
469 transformed response ratios of (b) CUE and (d) SOC. The response ratio is calculated as the
470 ratio of the measured value in treatment to the value in the control. Data are from meta-
471 analyses^{27, 41, 29}. Both datasets include observations from all three methods of CUE
472 measurement, i.e., C labeling, O labeling, and stoichiometry modeling as indicated by symbol
473 colors in panels a, b and c.

474

475 **Using models and data across scales to clarify the 476 microbial role in C cycling**

477 **Integrating genomic data with CUE and C models**

478 With the rise of high throughput sequencing technology, the use of genomic datasets to
479 help calibrate or validate C models has become both feasible and affordable. This capacity is
480 especially valuable when predicting CUE¹¹⁶. As genomic data related to microbial traits
481 becomes more readily available at both the population¹¹⁷ and community levels through
482 metagenomics¹¹⁸, there is a growing need to effectively integrate this data into C cycle models.
483 This integration requires models that can handle complex microbial interactions, from individual
484 populations to entire communities (Figure 2).

485 One way to integrate genomic data is by converting the genetic sequences of microbes
486 into information on metabolic pathways (e.g. cellulose degradation, lignin degradation, nitrogen
487 reduction, and fermentation) using genome-scale metabolic models (GEMs)¹¹⁹. GEMs take into
488 account the microbe's environment, such as substrate availability, and predict the
489 transformation of metabolites within a cell based on its genomic information. This process
490 allows for the calculation of CUE at the population level by analyzing substrate use and CO₂
491 production¹¹⁹. For community-level CUE, GEMs can be combined into microbial community
492 models that simulate interactions between different microbial taxa: The 'computation of
493 microbial ecosystems in time and space metabolic modeling platform' (COMETS) extends
494 GEMs to include dynamics of microbial growth and interactions, providing a tool for predicting
495 CUE_C under various environmental conditions¹¹⁶.

496 An alternative modeling approach at the community level is based on traits (e.g.,
497 quantity of cellulase produced, maximum rate of reaction (V_{max}) of cellulose decay by cellulase,
498 V_{max} of cellulose-monomer uptake, and turnover rate), such as the DEMENT model, which uses
499 data on microbial traits to simulate substrate use and CO_2 production¹²⁰. This model can predict
500 both CUE_P and CUE_C under different environmental conditions and over time. However,
501 translating genomic data into traits remains challenging¹²¹. Genomic datasets typically indicate
502 the presence or absence of certain genes or pathways, but additional information, such as that
503 from GEMs or experimental data, is necessary to accurately map these genes to functional
504 traits in the models.

505 Validating genomic and trait-based models is crucial and can be achieved using
506 community-level genomic datasets, which offer insights into microbial strategies that affect CUE,
507 such as nutrient recycling and stress tolerance^{118,122}. Combining these models with traditional
508 CUE measurements and omics data allows for the creation of detailed maps of community-level
509 CUE, offering new insights into C cycling dynamics and providing input information for C cycle
510 models.

511 A major challenge in this field is the high computational demand of integrating omic data
512 into complex models. One solution is the development of computational emulators that can
513 simulate the dynamics of microbial models more efficiently, bridging the gap between detailed,
514 small-scale models and broader applications in C cycle studies¹²³. This approach promises to
515 improve our understanding of microbial contributions to C cycling, leveraging the power of
516 genomic data to inform and validate complex ESMs.

517 Harmonization of CUE measurements and aligning measured and 518 modeled CUE

519 Harmonizing soil microbial CUE measurements across different methods, i.e., aligning
520 results from different methodologies, poses a challenge due to the differences across
521 measurement techniques. While adopting a universal protocol for CUE measurement—a single,
522 standardized measurement method—would be ideal, it may not be feasible given the
523 complexities of CUE. Therefore, a more practical approach involves providing a clear and
524 comprehensive description of the methodologies used in different studies. This detailed
525 reporting should include information on the physiological processes considered, such as
526 maintenance, enzyme production, biomass generation, and mortality rates. This level of detail

527 helps in understanding and comparing results across studies, as well as in selecting appropriate
528 data for model calibration ¹⁷.

529 In contemporary soil C models that explicitly incorporate microbial processes ^{25,85}, the
530 CUE is close to empirically measured CUE_C . To achieve a uniform approach to CUE
531 measurement, microbial models that resolve key processes influencing CUE, such as uptake,
532 respiration, exudation, and microbial death could be used ¹⁷. Such models can generate CUE
533 metrics that align with different measurement methodologies by incorporating a complete or
534 partial set of these processes into their calculations. Furthermore, these models can be adapted
535 to conduct numerical experiments with specific substrates or to incorporate isotopic tracers
536 (e.g., ^{13}C , ^{14}C , ^{18}O) to simulate outcomes from labeling experiments. This adaptability allows for
537 the exploration of hypotheses regarding discrepancies in measurements under diverse
538 conditions by modifying model boundary conditions. Additionally, microbial models serve as
539 foundational tools for integrating microbial metabolism into broader global C models, potentially
540 enhanced by machine learning emulators for improved scalability and applicability.

541 Constraining CUE using model-data fusion

542 Data assimilation encompasses a collection of techniques, including Bayesian inference,
543 that refine biogeochemical models by integrating observational data. This process not only
544 updates model parameters to reflect the most likely values based on available data but also
545 quantifies their uncertainties, thus bridging the gap between empirical observations and
546 theoretical models ¹⁰⁹. This approach is particularly valuable for parameters like microbial CUE,
547 which are challenging to measure directly in the field due to technical limitations. An innovative
548 application of data assimilation is demonstrated by Tao et al. ²¹, who developed the PROcess-
549 guided deep learning and DAta-driven (PRODA) approach ¹²⁴. This method integrates global-
550 scale SOC data with a microbially explicit model to produce a global map of microbial CUE.
551 PRODA employs traditional Bayesian data assimilation to estimate parameters at specific sites
552 and then uses deep learning to extrapolate these site-specific parameter estimates to a global
553 scale. The result is a set of parameters that optimally align with observed data, offering a
554 detailed view of microbial CUE and SOC storage patterns worldwide, along with other soil C
555 cycle dynamics such as decomposition rates, environmental impacts on soil respiration, and
556 vertical C transport ²¹.

557 Despite the potential of approaches like PRODA to harness large datasets for enhancing
558 our understanding of the soil C cycle, their computational intensity—stemming from the
559 extensive data sampling required by Bayesian inference—may limit their application in models
560 with complex structures. The next wave of data assimilation techniques will likely integrate
561 process-based models with deep learning algorithms more seamlessly ¹²². Such advancements
562 could offer quicker parameter optimization and facilitate comparisons across different models,
563 paving the way for more accurate and comprehensive assessments of microbial CUE and C
564 cycle dynamics on a global scale.

565 Long-term SOC records and ecosystem manipulation experiments

566 Ecosystem manipulation experiments and observations of natural gradients offer
567 invaluable insights into how microbial communities and CUE adapt to global change factors.
568 Especially insightful are field experiments (or studies leveraging natural gradients) that alter
569 environmental factors such as soil temperature, precipitation patterns, or nutrient levels ^{79,126}
570 over long durations. These experiments provide critical data on the enduring effects of global
571 change drivers on CUE, while simultaneously highlighting the limitations of current models and
572 enhancing our comprehension of ecological processes. Integrating the results from these
573 experiments with model simulations, supported by proven site modeling protocols and extra
574 observational data, is crucial for steadily enhancing the accuracy and complexity of models ¹²⁷.

575 Incorporating radiocarbon (¹⁴C) data and long-term SOC records into models is also vital
576 for refining CUE forecasts across longer (decadal to centennial) time scales. This temporal
577 information is essential for capturing the dynamics of CUE over time, thereby improving the
578 precision of models in depicting spatial and temporal fluctuations ¹²⁸.

579 Diagnosing CUE from existing models or simulation archives

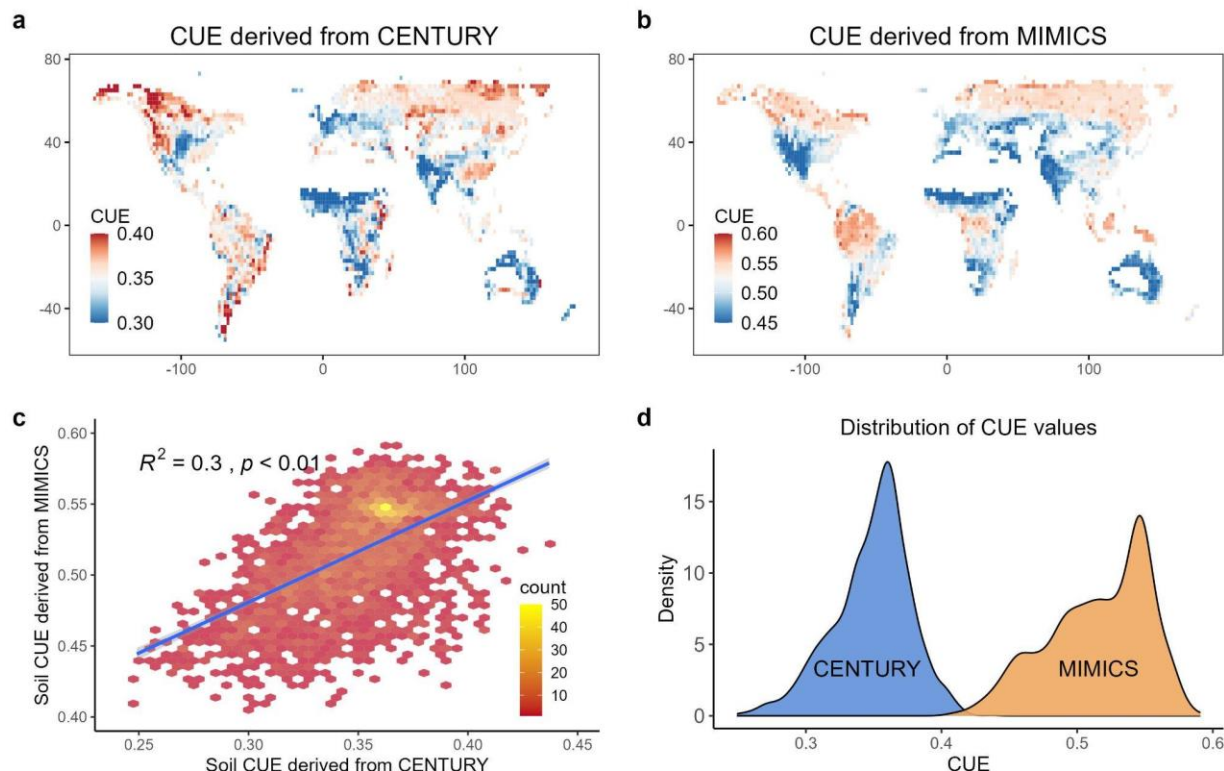
580 In global C modeling, approaches to quantify the environmental impact on organic
581 matter decomposition and stabilization differ significantly. An effective method for estimating
582 microbial CUE at the ecosystem level as emerging from model simulations involves the
583 calculation of the ratio between soil heterotrophic respiration (R) and gross decomposition (D)
584 within these models. Gross decomposition refers to the sum of all C fluxes transferred between
585 the modeled soil C pools that are mediated by microbial processes, excluding physically
586 mediated transfers (e.g., sorption, aggregation, or leaching). This includes all C removed from

587 organic matter pools, whether it is lost as CO₂ or transferred to another pool (SI-Text 1). This
588 ratio effectively quantifies microbial-mediated C losses from SOC pools, integrating both growth
589 (anabolic processes) and respiration (catabolic processes). Under steady-state conditions, it is
590 assumed that heterotrophic respiration aligns with microbial C uptake, resulting in the formula:
591 CUE = 1 - R/D. The steady-state assumption implies that microbial communities and SOC stock
592 are stable in time (i.e., in equilibrium with boundary conditions). This is an approximation of real
593 systems where SOC varies due to anthropogenic and natural changes (e.g., Holocene climatic
594 variations). This diagnosed CUE, emerging as a property inherent to the model, is not
595 susceptible to the equifinality issues that can affect the underlying intrinsic model parameters
596 (like CUE_E), and it does not necessitate the incorporation of explicitly microbial models, offering
597 a simplified yet insightful metric. These model-based CUE estimates, derived from long-term
598 flux averages (e.g., 20 years), represent stable C stocks. In contrast, measurement-based
599 estimates, taken over shorter periods, are more susceptible to significant CUE variations due to
600 asynchronous fluctuations in components such as respiration and degradation, potentially
601 introducing estimation inaccuracies. This timescale discrepancy likely accounts for the greater
602 variability observed in measurement-based CUE compared to model-based CUE. We propose
603 this "model-diagnosed CUE" as a novel metric, designed to estimate microbial CUE from model
604 outputs without direct measurements of microbial uptake.

605 Analyzing diagnosed CUE and its relationship with SOC across various models, such as
606 those evaluated in the Trends in the land carbon cycle (TRENDY) model intercomparison
607 project², facilitates the identification of differences attributable to unique model structures and
608 assumptions. For example, warming-induced CO₂ emissions should be higher in models with
609 low diagnosed CUE compared to high CUE as the warming-induced stimulation of microbial
610 activity will result in relatively more C being respired than cycled within the soil systems. This
611 approach further allows the benchmarking and subsequent refinement of diagnosed CUE
612 estimates using observed CUE_E data.

613 For instance, we derived CUE estimates from simulations conducted with two different
614 versions of the Organising Carbon and Hydrology In Dynamic Ecosystems (ORCHIDEE) land
615 surface model¹²⁹, which differ in the SOC model deployed. The CENTURY SOC model (Fig.
616 S1a), which is widely used but does not resolve microbial processes, uses first-order decay,
617 while the MIMICS model (Fig. S1b) resolves microbial physiology, providing a more mechanistic
618 understanding of microbial processes. The resulting global CUE maps (the average of
619 simulation results over 20 consecutive years) revealed significant spatial variability (Fig. 6a & b).

620 While the two maps showed a good correlation (Fig. 6c), the CUE values diagnosed from the
 621 MIMICS model were higher than those from the CENTURY model (Fig. 6d). These findings
 622 underscore the importance of incorporating observational data into model calibration efforts to
 623 enhance the accuracy and reliability of SOC predictions by realistically resolving CUE.



624
 625 **Figure 6. Diagnosed CUE from two existing soil C models.** CUE diagnosed from a nutrient-
 626 enabled version of the the Organising Carbon and Hydrology In Dynamic Ecosystems land
 627 surface model (ORCHIDEE-CNP) deploying a soil module based on (a) the CENTURY model
 628 ¹²⁹, or (b) the MIMICS model with constant intrinsic CUE_C ¹³⁰. (c) Correlation between diagnosed
 629 CUE values from the CENTURY-based model and the MIMICS-based model. (d) Distribution
 630 frequency of CUE for the two scenarios.

631

632 In conclusion, the inherent structure of a model significantly shapes its outcomes,
 633 making the integration of empirical data with data-constrained models a fundamental step
 634 toward realistic predictions ^{131,132}. Precisely delineating the spatial and temporal dynamics of
 635 CUE in models that specifically address microbial activities is crucial for the reliability of their
 636 predictions of SOC status and dynamics. Moreover, future soil C models must navigate the

637 intricate balance between the complex regulatory mechanisms of CUE, other processes
638 governing SOC formation and stabilization, and the practicality of model use to promote more
639 precise projections of CUE responses under diverse environmental scenarios. This Perspective
640 underscores the importance of combining different data sources with sophisticated modeling
641 techniques to refine global CUE predictions. By incorporating genomic data, standardizing
642 measurement protocols, applying data assimilation practices and critically evaluating CUE
643 within existing frameworks, our comprehension of the global dynamics of microbial CUE can be
644 markedly improved. This Perspective provides a roadmap for establishing an effective modeling
645 approach to accurately represent global soil microbial CUE and its interactions with other
646 biological and abiotic processes that regulate SOC dynamics.

647

648

649 **Reference:**

- 650 1. Eyring, V. *et al.* Overview of the Coupled Model Intercomparison Project Phase 6 (CMIP6)
651 experimental design and organization. *Geosci. Model Dev.* **9**, 1937–1958 (2016).
- 652 2. Friedlingstein, P. *et al.* Global Carbon Budget 2023. *Earth Syst. Sci. Data* **15**, 5301–5369
653 (2023).
- 654 3. Shi, Z. *et al.* Global-Scale Convergence Obscures Inconsistencies in Soil Carbon Change
655 Predicted by Earth System Models. *AGU Adv.* **5**, e2023AV001068 (2024).
- 656 4. Varney, R. M., Chadburn, S. E., Burke, E. J. & Cox, P. M. Evaluation of soil carbon
657 simulation in CMIP6 Earth system models. *Biogeosciences* **19**, 4671–4704 (2022).
- 658 5. Crowther, T. W. *et al.* The global soil community and its influence on biogeochemistry.
659 *Science* **365**, eaav0550 (2019).
- 660 6. Ranheim Sveen, T., Hannula, S. E. & Bahram, M. Microbial regulation of feedbacks to
661 ecosystem change. *Trends Microbiol.* S0966842X23001919 (2023)
662 doi:10.1016/j.tim.2023.06.006.
- 663 7. Fierer, N. Embracing the unknown: disentangling the complexities of the soil microbiome.

664 *Nat. Rev. Microbiol.* **15**, 579–590 (2017).

665 8. Manzoni, S., Taylor, P., Richter, A., Porporato, A. & Ågren, G. I. Environmental and
666 stoichiometric controls on microbial carbon-use efficiency in soils. *New Phytol.* **196**, 79–91
667 (2012).

668 9. Allison, S. D., Wallenstein, M. D. & Bradford, M. A. Soil-carbon response to warming
669 dependent on microbial physiology. *Nat. Geosci.* **3**, 336–340 (2010).

670 10. Domeignoz-Horta, L. A. *et al.* Microbial diversity drives carbon use efficiency in a model
671 soil. *Nat. Commun.* **11**, 3684 (2020).

672 11. Karhu, K. *et al.* Temperature sensitivity of soil respiration rates enhanced by microbial
673 community response. *Nature* **513**, 81–84 (2014).

674 12. Luo, Z. *et al.* Convergent modelling of past soil organic carbon stocks but divergent
675 projections. *Biogeosciences* **12**, 4373–4383 (2015).

676 13. Wieder, W. R., Cleveland, C. C., Smith, W. K. & Todd-Brown, K. Future productivity and
677 carbon storage limited by terrestrial nutrient availability. *Nat. Geosci.* **8**, 441–444 (2015).

678 14. Geyer, K. M., Kyker-Snowman, E., Grandy, A. S. & Frey, S. D. Microbial carbon use
679 efficiency: accounting for population, community, and ecosystem-scale controls over the
680 fate of metabolized organic matter. *Biogeochemistry* **127**, 173–188 (2016).

681 15. Treseder, K. K. *et al.* Integrating microbial ecology into ecosystem models: challenges and
682 priorities. *Biogeochemistry* **109**, 7–18 (2012).

683 16. Manzoni, S. *et al.* Reviews and syntheses: Carbon use efficiency from organisms to
684 ecosystems – definitions, theories, and empirical evidence. *Biogeosciences* **15**, 5929–
685 5949 (2018).

686 17. Dijkstra, P. *et al.* On maintenance and metabolisms in soil microbial communities. *Plant
687 Soil* **476**, 385–396 (2022).

688 18. Hagerty, S. B., Allison, S. D. & Schimel, J. P. Evaluating soil microbial carbon use

689 efficiency explicitly as a function of cellular processes: implications for measurements and
690 models. *Biogeochemistry* **140**, 269–283 (2018).

691 19. He, P., Zhang, Y., Shen, Q., Ling, N. & Nan, Z. Microbial carbon use efficiency in different
692 ecosystems: A meta-analysis based on a biogeochemical equilibrium model. *Glob.*
693 *Change Biol.* **00**, 1–17 (2023).

694 20. Qiao, Y. *et al.* Global variation of soil microbial carbon-use efficiency in relation to growth
695 temperature and substrate supply. *Sci. Rep.* **9**, 5621 (2019).

696 21. Tao, F. *et al.* Microbial carbon use efficiency promotes global soil carbon storage. *Nature*
697 (2023) doi:10.1038/s41586-023-06042-3.

698 22. Manzoni, S. Flexible Carbon-Use Efficiency across Litter Types and during Decomposition
699 Partly Compensates Nutrient Imbalances—Results from Analytical Stoichiometric Models.
700 *Front. Microbiol.* **8**, 661 (2017).

701 23. Wieder, W. R., Bonan, G. B. & Allison, S. D. Global soil carbon projections are improved
702 by modelling microbial processes. *Nat. Clim. Change* **3**, 909–912 (2013).

703 24. Zhang, H. *et al.* Modeling the effects of litter stoichiometry and soil mineral N availability on
704 soil organic matter formation using CENTURY-CUE (v1.0). *Geosci. Model Dev.* **11**, 4779–
705 4796 (2018).

706 25. Wieder, W. R., Grandy, A. S., Kallenbach, C. M. & Bonan, G. B. Integrating microbial
707 physiology and physio-chemical principles in soils with the Microbial-MIneral Carbon
708 Stabilization (MIMICS) model. *Biogeosciences* **11**, 3899–3917 (2014).

709 26. Sulman, B. N., Phillips, R. P., Oishi, A. C., Shevliakova, E. & Pacala, S. W. Microbe-driven
710 turnover offsets mineral-mediated storage of soil carbon under elevated CO₂. *Nat. Clim.*
711 *Change* **4**, 1099–1102 (2014).

712 27. He, X. *et al.* Model uncertainty obscures major driver of soil carbon. *Nature* **627**, E1–E3
713 (2024).

714 28. Shi, Z., Crowell, S., Luo, Y. & Moore, B. Model structures amplify uncertainty in predicted

715 soil carbon responses to climate change. *Nat. Commun.* **9**, 2171 (2018).

716 29. Wu, J., Cheng, X. & Liu, G. Increased soil organic carbon response to fertilization is
717 associated with increasing microbial carbon use efficiency: Data synthesis. *Soil Biol.*
718 *Biochem.* **171**, 108731 (2022).

719 30. Islam, Md. R., Singh, B. & Dijkstra, F. A. Microbial carbon use efficiency of glucose varies
720 with soil clay content: A meta-analysis. *Appl. Soil Ecol.* **181**, 104636 (2023).

721 31. Schnecker, J. *et al.* Seasonal dynamics of soil microbial growth, respiration, biomass, and
722 carbon use efficiency in temperate soils. *Geoderma* **440**, 116693 (2023).

723 32. Wieder, W. R., Grandy, A. S., Kallenbach, C. M., Taylor, P. G. & Bonan, G. B.
724 Representing life in the Earth system with soil microbial functional traits in the MIMICS
725 model. *Geosci. Model Dev.* **8**, 1789–1808 (2015).

726 33. Sinsabaugh, R. L. *et al.* Stoichiometry of microbial carbon use efficiency in soils. *Ecol.*
727 *Monogr.* **86**, 172–189 (2016).

728 34. Camenzind, T., Mason-Jones, K., Mansour, I., Rillig, M. C. & Lehmann, J. Formation of
729 necromass-derived soil organic carbon determined by microbial death pathways. *Nat.*
730 *Geosci.* **16**, 115–122 (2023).

731 35. Frey, S. D., Lee, J., Melillo, J. M. & Six, J. The temperature response of soil microbial
732 efficiency and its feedback to climate. *Nat. Clim. Change* **3**, 395–398 (2013).

733 36. Spohn, M., Klaus, K., Wanek, W. & Richter, A. Microbial carbon use efficiency and
734 biomass turnover times depending on soil depth – Implications for carbon cycling. *Soil Biol.*
735 *Biochem.* **96**, 74–81 (2016).

736 37. Sinsabaugh, R. L., Manzoni, S., Moorhead, D. L. & Richter, A. Carbon use efficiency of
737 microbial communities: stoichiometry, methodology and modelling. *Ecol. Lett.* **16**, 930–939
738 (2013).

739 38. Zhang, Q., Qin, W., Feng, J. & Zhu, B. Responses of soil microbial carbon use efficiency to
740 warming: Review and prospects. *Soil Ecol. Lett.* **4**, 307–318 (2022).

741 39. Geyer, K. M., Dijkstra, P., Sinsabaugh, R. & Frey, S. D. Clarifying the interpretation of
742 carbon use efficiency in soil through methods comparison. *Soil Biol. Biochem.* **128**, 79–88
743 (2019).

744 40. Schimel, J., Weintraub, M. N. & Moorhead, D. Estimating microbial carbon use efficiency in
745 soil: Isotope-based and enzyme-based methods measure fundamentally different aspects
746 of microbial resource use. *Soil Biol. Biochem.* **169**, 108677 (2022).

747 41. Hu, J., Huang, C., Zhou, S. & Kuzyakov, Y. Nitrogen addition to soil affects microbial
748 carbon use efficiency: Meta-analysis of similarities and differences in ^{13}C and ^{18}O
749 approaches. *Glob. Change Biol.* **28**, 4977–4988 (2022).

750 42. Hagerty, S. B. *et al.* Accelerated microbial turnover but constant growth efficiency with
751 warming in soil. *Nat. Clim. Change* **4**, 903–906 (2014).

752 43. Simon, E. *et al.* Microbial growth and carbon use efficiency show seasonal responses in a
753 multifactorial climate change experiment. *Commun. Biol.* **3**, 584 (2020).

754 44. Qu, L., Wang, C. & Bai, E. Evaluation of the ^{18}O - H_2O incubation method for measurement
755 of soil microbial carbon use efficiency. *Soil Biol. Biochem.* **145**, 107802 (2020).

756 45. Canarini, A. *et al.* Quantifying microbial growth and carbon use efficiency in dry soil
757 environments via ^{18}O water vapor equilibration. *Glob. Change Biol.* **26**, 5333–5341 (2020).

758 46. Sun, L. *et al.* Interpreting the differences in microbial carbon and nitrogen use efficiencies
759 estimated by ^{18}O labeling and ecoenzyme stoichiometry. *Geoderma* **444**, 116856 (2024).

760 47. Yang, S. *et al.* Enhancing insights: exploring the information content of calorespirometric
761 ratio in dynamic soil microbial growth processes through calorimetry. *Front. Microbiol.* **15**,
762 1321059 (2024).

763 48. Fewster, R. E. *et al.* Imminent loss of climate space for permafrost peatlands in Europe
764 and Western Siberia. *Nat. Clim. Change* **12**, 373–379 (2022).

765 49. Hugelius, G. *et al.* Large stocks of peatland carbon and nitrogen are vulnerable to

766 permafrost thaw. *Proc. Natl. Acad. Sci.* **117**, 20438–20446 (2020).

767 50. Takriti, M. *et al.* Soil organic matter quality exerts a stronger control than stoichiometry on
768 microbial substrate use efficiency along a latitudinal transect. *Soil Biol. Biochem.* **121**, 212–
769 220 (2018).

770 51. Zhang, Q. *et al.* Whole-soil-profile warming does not change microbial carbon use
771 efficiency in surface and deep soils. *Proc. Natl. Acad. Sci.* **120**, e2302190120 (2023).

772 52. Jiang, Y. *et al.* Deep soil microbial carbon use efficiency responds stronger to nitrogen
773 deposition than top soil in tropical forests, southern China. *Plant Soil* (2024)
774 doi:10.1007/s11104-024-06509-w.

775 53. Brangarí, A. C., Manzoni, S. & Rousk, J. A soil microbial model to analyze decoupled
776 microbial growth and respiration during soil drying and rewetting. *Soil Biol. Biochem.* **148**,
777 107871 (2020).

778 54. Li, X., Leizeaga, A., Rousk, J., Hugelius, G. & Manzoni, S. Drying intensity and acidity slow
779 down microbial growth recovery after rewetting dry soils. *Soil Biol. Biochem.* **184**, 109115
780 (2023).

781 55. Couradeau, E. *et al.* Probing the active fraction of soil microbiomes using BONCAT-FACS.
782 *Nat. Commun.* **10**, 2770 (2019).

783 56. Blagodatskaya, E. & Kuzyakov, Y. Active microorganisms in soil: Critical review of
784 estimation criteria and approaches. *Soil Biol. Biochem.* **67**, 192–211 (2013).

785 57. Hasby, F. A., Barbi, F., Manzoni, S. & Lindahl, B. D. Transcriptomic markers of fungal
786 growth, respiration and carbon-use efficiency. *FEMS Microbiol. Lett.* **368**, fnab100 (2021).

787 58. Khurana, S. *et al.* Interactive effects of microbial functional diversity and carbon availability
788 on decomposition – A theoretical exploration. *Ecol. Model.* **486**, 110507 (2023).

789 59. Anthony, M. A., Crowther, T. W., Maynard, D. S., Van Den Hoogen, J. & Averill, C. Distinct
790 Assembly Processes and Microbial Communities Constrain Soil Organic Carbon
791 Formation. *One Earth* **2**, 349–360 (2020).

792 60. Soares, M. & Rousk, J. Microbial growth and carbon use efficiency in soil: Links to fungal-
793 bacterial dominance, SOC-quality and stoichiometry. *Soil Biol. Biochem.* **131**, 195–205
794 (2019).

795 61. Malik, A. A. *et al.* Soil Fungal:Bacterial Ratios Are Linked to Altered Carbon Cycling. *Front.*
796 *Microbiol.* **7**, (2016).

797 62. Keiblunger, K. M. *et al.* The effect of resource quantity and resource stoichiometry on
798 microbial carbon-use-efficiency: Resource quantity/quality drives microbial C-use-
799 efficiency. *FEMS Microbiol. Ecol.* no-no (2010) doi:10.1111/j.1574-6941.2010.00912.x.

800 63. Six, J., Frey, S. D., Thiet, R. K. & Batten, K. M. Bacterial and Fungal Contributions to
801 Carbon Sequestration in Agroecosystems. *Soil Sci. Soc. Am. J.* **70**, 555–569 (2006).

802 64. Ma, S., Zhu, W., Wang, W., Li, X. & Sheng, Z. Microbial assemblies with distinct trophic
803 strategies drive changes in soil microbial carbon use efficiency along vegetation primary
804 succession in a glacier retreat area of the southeastern Tibetan Plateau. *Sci. Total*
805 *Environ.* **867**, 161587 (2023).

806 65. Allison, S. D. Modeling adaptation of carbon use efficiency in microbial communities. *Front.*
807 *Microbiol.* **5**, (2014).

808 66. Qu, L. *et al.* Stronger compensatory thermal adaptation of soil microbial respiration with
809 higher substrate availability. *ISME J.* wrae025 (2024) doi:10.1093/ismejo/wrae025.

810 67. Kaiser, C., Franklin, O., Dieckmann, U. & Richter, A. Microbial community dynamics
811 alleviate stoichiometric constraints during litter decay. *Ecol. Lett.* **17**, 680–690 (2014).

812 68. Brangarí, A. C., Manzoni, S. & Rousk, J. The mechanisms underpinning microbial
813 resilience to drying and rewetting – A model analysis. *Soil Biol. Biochem.* **162**, 108400
814 (2021).

815 69. Maynard, D. S., Crowther, T. W. & Bradford, M. A. Fungal interactions reduce carbon use
816 efficiency. *Ecol. Lett.* **20**, 1034–1042 (2017).

817 70. Iven, H., Walker, T. W. N. & Anthony, M. Biotic Interactions in Soil are Underestimated

818 Drivers of Microbial Carbon Use Efficiency. *Curr. Microbiol.* **80**, 13 (2023).

819 71. Frey, S. D. Protozoan grazing affects estimates of carbon utilization efficiency of the soil
820 microbial community. *Soil Biol. Biochem.* (2001).

821 72. Ma, L. *et al.* Long-term conservation tillage enhances microbial carbon use efficiency by
822 altering multitrophic interactions in soil. *Sci. Total Environ.* **915**, 170018 (2024).

823 73. Tian, W. *et al.* Thermal adaptation occurs in the respiration and growth of widely distributed
824 bacteria. *Glob. Change Biol.* **28**, 2820–2829 (2022).

825 74. Pold, G. *et al.* Carbon Use Efficiency and Its Temperature Sensitivity Covary in Soil
826 Bacteria. *mBio* **11**, e02293-19 (2020).

827 75. Tian, J. *et al.* Microbially mediated mechanisms underlie soil carbon accrual by
828 conservation agriculture under decade-long warming. *Nat. Commun.* **15**, 377 (2024).

829 76. Walker, T. W. N. *et al.* Microbial temperature sensitivity and biomass change explain soil
830 carbon loss with warming. *Nat. Clim. Change* **8**, 885–889 (2018).

831 77. Kallenbach, C. M., Wallenstein, M. D., Schipanksi, M. E. & Grandy, A. S. Managing
832 Agroecosystems for Soil Microbial Carbon Use Efficiency: Ecological Unknowns, Potential
833 Outcomes, and a Path Forward. *Front. Microbiol.* **10**, 1146 (2019).

834 78. Ye, J., Bradford, M. A., Maestre, F. T., Li, F. & García-Palacios, P. Compensatory Thermal
835 Adaptation of Soil Microbial Respiration Rates in Global Croplands. *Glob. Biogeochem.*
836 *Cycles* **34**, (2020).

837 79. Metze, D. *et al.* Soil warming increases the number of growing bacterial taxa but not their
838 growth rates. *Sci. Adv.* **10**, eadk6295 (2024).

839 80. Saifuddin, M., Bhatnagar, J. M., Segrè, D. & Finzi, A. C. Microbial carbon use efficiency
840 predicted from genome-scale metabolic models. *Nat. Commun.* **10**, 3568 (2019).

841 81. Smith, T. P., Clegg, T., Bell, T. & Pawar, S. Systematic variation in the temperature
842 dependence of bacterial carbon use efficiency. *Ecol. Lett.* **24**, 2123–2133 (2021).

843 82. Sun, Y. *et al.* A global meta-analysis on the responses of C and N concentrations to
844 warming in terrestrial ecosystems. *CATENA* **208**, 105762 (2022).

845 83. Xu, W. *et al.* A meta-analysis of the response of soil moisture to experimental warming.
846 *Environ. Res. Lett.* **8**, 044027 (2013).

847 84. Fuchslueger, L. *et al.* Microbial carbon and nitrogen cycling responses to drought and
848 temperature in differently managed mountain grasslands. *Soil Biol. Biochem.* **135**, 144–
849 153 (2019).

850 85. Abramoff, R. Z. *et al.* Improved global-scale predictions of soil carbon stocks with Millennial
851 Version 2. *Soil Biol. Biochem.* **164**, 108466 (2022).

852 86. Zheng, Q. *et al.* Growth explains microbial carbon use efficiency across soils differing in
853 land use and geology. *Soil Biol. Biochem.* **128**, 45–55 (2019).

854 87. Metze, D. *et al.* Microbial growth under drought is confined to distinct taxa and modified by
855 potential future climate conditions. *Nat. Commun.* **14**, 5895 (2023).

856 88. Manzoni, S. Optimal metabolic regulation along resource stoichiometry gradients. *Ecol.*
857 *Lett.* (2017).

858 89. Mason-Jones, K., Breidenbach, A., Dyckmans, J., Banfield, C. C. & Dippold, M. A.
859 Intracellular carbon storage by microorganisms is an overlooked pathway of biomass
860 growth. *Nat. Commun.* **14**, 2240 (2023).

861 90. Jones, D. L., Cooledge, E. C., Hoyle, F. C., Griffiths, R. I. & Murphy, D. V. pH and
862 exchangeable aluminum are major regulators of microbial energy flow and carbon use
863 efficiency in soil microbial communities. *Soil Biol. Biochem.* **138**, 107584 (2019).

864 91. Malik, A. A. *et al.* Land use driven change in soil pH affects microbial carbon cycling
865 processes. *Nat. Commun.* **9**, 3591 (2018).

866 92. Silva-Sánchez, A., Soares, M. & Rousk, J. Testing the dependence of microbial growth
867 and carbon use efficiency on nitrogen availability, pH, and organic matter quality. *Soil Biol.*
868 *Biochem.* **134**, 25–35 (2019).

869 93. Zhang, X. *et al.* Erosion effects on soil microbial carbon use efficiency in the mollisol
870 cropland in northeast China. *Soil Ecol. Lett.* **5**, 230176 (2023).

871 94. Schroeder, J. *et al.* Liming effects on microbial carbon use efficiency and its potential
872 consequences for soil organic carbon stocks. *Soil Biol. Biochem.* **191**, 109342 (2024).

873 95. Schmidt, M. W. I. *et al.* Persistence of soil organic matter as an ecosystem property.
874 *Nature* **478**, 49–56 (2011).

875 96. Young, I. M. & Crawford, J. W. Interactions and Self-Organization in the Soil-Microbe
876 Complex. *Science* **304**, 1634–1637 (2004).

877 97. Kuzyakov, Y. & Blagodatskaya, E. Microbial hotspots and hot moments in soil: Concept &
878 review. *Soil Biol. Biochem.* **83**, 184–199 (2015).

879 98. Cai, Y. *et al.* Assessing the accumulation efficiency of various microbial carbon
880 components in soils of different minerals. *Geoderma* **407**, 115562 (2022).

881 99. Jeewani, P. H. *et al.* The stoichiometric C-Fe ratio regulates glucose mineralization and
882 stabilization via microbial processes. *Geoderma* **383**, 114769 (2021).

883 100. Bölscher, T., Wadsö, L., Börjesson, G. & Herrmann, A. M. Differences in substrate use
884 efficiency: impacts of microbial community composition, land use management, and
885 substrate complexity. *Biol. Fertil. Soils* **52**, 547–559 (2016).

886 101. Jones, D. L. *et al.* Role of substrate supply on microbial carbon use efficiency and its role
887 in interpreting soil microbial community-level physiological profiles (CLPP). *Soil Biol.*
888 *Biochem.* **123**, 1–6 (2018).

889 102. Chakrawal, A., Calabrese, S., Herrmann, A. M. & Manzoni, S. Interacting Bioenergetic and
890 Stoichiometric Controls on Microbial Growth. *Front. Microbiol.* **13**, 859063 (2022).

891 103. Kleerebezem, R. & Van Loosdrecht, M. C. M. A Generalized Method for Thermodynamic
892 State Analysis of Environmental Systems. *Crit. Rev. Environ. Sci. Technol.* **40**, 1–54
893 (2010).

894 104. Cotrufo, M. F., Wallenstein, M. D., Boot, C. M., Denef, K. & Paul, E. The Microbial

895 Efficiency-Matrix Stabilization (MEMS) framework integrates plant litter decomposition with
896 soil organic matter stabilization: do labile plant inputs form stable soil organic matter? *Glob.*
897 *Change Biol.* **19**, 988–995 (2013).

898 105. Craig, M. E. *et al.* Fast-decaying plant litter enhances soil carbon in temperate forests but
899 not through microbial physiological traits. *Nat. Commun.* **13**, 1229 (2022).

900 106. Sokol, N. W. *et al.* The path from root input to mineral-associated soil carbon is shaped by
901 habitat-specific microbial traits and soil moisture. *Soil Biol. Biochem.* 109367 (2024)
902 doi:10.1016/j.soilbio.2024.109367.

903 107. Liang, C., Schimel, J. P. & Jastrow, J. D. The importance of anabolism in microbial control
904 over soil carbon storage. *Nat. Microbiol.* **2**, 17105 (2017).

905 108. Li, Z. *et al.* Microbial metabolic capacity regulates the accrual of mineral-associated
906 organic carbon in subtropical paddy soils. *Soil Biol. Biochem.* 109457 (2024)
907 doi:10.1016/j.soilbio.2024.109457.

908 109. Luo, Y. & Schuur, E. A. G. Model parameterization to represent processes at unresolved
909 scales and changing properties of evolving systems. *Glob. Change Biol.* **26**, 1109–1117
910 (2020).

911 110. Kallenbach, C. M., Frey, S. D. & Grandy, A. S. Direct evidence for microbial-derived soil
912 organic matter formation and its ecophysiological controls. *Nat. Commun.* **7**, 13630 (2016).

913 111. Xiao, K.-Q. *et al.* Beyond microbial carbon use efficiency. *Natl. Sci. Rev.* nwae059 (2024)
914 doi:10.1093/nsr/nwae059.

915 112. Georgiou, K. *et al.* Global stocks and capacity of mineral-associated soil organic carbon.
916 *Nat. Commun.* **13**, 3797 (2022).

917 113. Zhu, E. *et al.* Enhanced Mineral Preservation Rather Than Microbial Residue Production
918 Dictates the Accrual of Mineral-Associated Organic Carbon Along a Weathering Gradient.
919 *Geophys. Res. Lett.* **51**, e2024GL108466 (2024).

920 114. García-Palacios, P. *et al.* Dominance of particulate organic carbon in top mineral soils in
921 cold regions. *Nat. Geosci.* (2024) doi:10.1038/s41561-023-01354-5.

922 115. Lí, J. *et al.* Subarctic winter warming promotes soil microbial resilience to freeze–thaw
923 cycles and enhances the microbial carbon use efficiency. *Glob. Change Biol.* **30**, e17040
924 (2024).

925 116. Dukovski, I. *et al.* A metabolic modeling platform for the computation of microbial
926 ecosystems in time and space (COMETS). *Nat. Protoc.* **16**, 5030–5082 (2021).

927 117. Karaoz, U. & Brodie, E. L. microTrait: A Toolset for a Trait-Based Representation of
928 Microbial Genomes. *Front. Bioinforma.* **2**, 918853 (2022).

929 118. Piton, G. *et al.* Life history strategies of soil bacterial communities across global terrestrial
930 biomes. *Nat. Microbiol.* **8**, 2093–2102 (2023).

931 119. Gu, C., Kim, G. B., Kim, W. J., Kim, H. U. & Lee, S. Y. Current status and applications of
932 genome-scale metabolic models. *Genome Biol.* **20**, 121 (2019).

933 120. Abs, E., Albright, M. B. N. & Allison, S. D. Invasions eliminate the legacy effects of
934 substrate history on microbial nitrogen cycling. *Ecosphere* **15**, e4754 (2024).

935 121. Bernstein, D. B., Sulheim, S., Almaas, E. & Segrè, D. Addressing uncertainty in genome-
936 scale metabolic model reconstruction and analysis. *Genome Biol.* **22**, 64 (2021).

937 122. Malik, A. A. *et al.* Defining trait-based microbial strategies with consequences for soil
938 carbon cycling under climate change. *ISME J.* **14**, 1–9 (2020).

939 123. Demirer, E. *et al.* Improving the Performance of Reactive Transport Simulations Using
940 Artificial Neural Networks. *Transp. Porous Media* **149**, 271–297 (2023).

941 124. Tao, F. *et al.* Deep Learning Optimizes Data-Driven Representation of Soil Organic Carbon
942 in Earth System Model Over the Conterminous United States. *Front. Big Data* **3**, 17 (2020).

943 125. Reichstein, M. *et al.* Deep learning and process understanding for data-driven Earth
944 system science. *Nature* **566**, 195–204 (2019).

945 126. Song, J. *et al.* A meta-analysis of 1,119 manipulative experiments on terrestrial carbon-

946 cycling responses to global change. *Nat. Ecol. Evol.* **3**, 1309–1320 (2019).

947 127. Norby, R. J. *et al.* Model–data synthesis for the next generation of forest free-air CO₂

948 enrichment (FACE) experiments. *New Phytol.* **209**, 17–28 (2016).

949 128. Tifafi, M. *et al.* The use of radiocarbon 14C to constrain carbon dynamics in the soil

950 module of the land surface model ORCHIDEE (SVN r5165). *Geosci. Model Dev.* **11**, 4711–

951 4726 (2018).

952 129. Goll, D. S. *et al.* A representation of the phosphorus cycle for ORCHIDEE (revision 4520).

953 *Geosci. Model Dev.* **10**, 3745–3770 (2017).

954 130. Zhang, H. *et al.* Microbial dynamics and soil physicochemical properties explain large-

955 scale variations in soil organic carbon. *Glob. Change Biol.* **26**, 2668–2685 (2020).

956 131. Luo, Y. *et al.* Toward more realistic projections of soil carbon dynamics by Earth system

957 models. *Glob. Biogeochem. Cycles* **30**, 40–56 (2016).

958 132. Tao, F. *et al.* Convergence in simulating global soil organic carbon by structurally different

959 models after data assimilation. *Glob. Change Biol.* **30**, e17297 (2024).

960

961 **Acknowledgement:**

962 This work received support from the CALIPSO project provided by Schmidt Sciences. DSG, XH
963 and NN acknowledge support from the EJP Soil ICONICA project. Funding to EA was provided
964 by the European Union's Horizon 2020 research and innovation programme under the Marie
965 Skłodowska-Curie (Grant Agreement No. 891576). SPKB was funded by research project
966 FirEURisk, a European Union Horizon 2020 research and innovation program (Grant Agreement
967 No. 101003890). KG was supported by the LLNL LDRD Program under the auspices of DOE
968 Contract DE-AC52-07NA27344. The contribution of LE was co-funded by the EJP Soil project
969 CarboSeq, which has received funding from the European Union's Horizon 2020 Research and
970 Innovation Programme (Grant Agreement No. 862695). SM has received funding from the
971 European Research Council (ERC) under the European Union's Horizon 2020 research and
972 innovation programme (Grant Agreement No. 101001608).

973

974 **Competing interests**

975 The authors declare no competing interests.

976

977 **Author contributions**

978 X.H. and D.S.G. initiated the writing and led the design and writing of the article. S.A., S.M.,
979 P.C., G.H., K.G., Y.L., N.N., and Y.W. participated in the initial design of the content. E.A. and
980 S.A. drafted section 4.1. F.T. and Y.H. drafted section 4.3. R.A., E.B., S.P.K.B., A.C., L.E., P.F.,
981 L.B.H., W.L., G.M., C.Q., and S.S. provided input on the manuscript text, figures and discussion
982 of scientific content.

983